

# Performance of a Virtual Conductor in Dc Power Systems Using a Controlled Bidirectional DC-DC Converter

Husam A. Ramadan<sup>1</sup>, Yasutaka Imamura<sup>2</sup>, Sihun Yang<sup>3</sup>, Masahito Shoyama<sup>4</sup>

Kyushu University, Fukuoka, 819-0395 Japan<sup>1,2,3,4</sup>

**Abstract:** This paper proposes a new control strategy for bidirectional DC-DC converter. This strategy aims at controlling a bidirectional DC-DC converter to behave like a virtual conductor. As a matter of fact, the voltage difference between the terminals of any conductor is zero volts. Conversely, the main target of this proposed control strategy is to keep the voltage difference between the converter terminals constant at a certain value. In other words, this strategy permits the DC-DC converter to transfer the power between two nodes at different voltage levels. In this way, the converter performs like a conductor, but unlike the normal conductor, has a voltage difference between its terminals. Thus, the authors call it a virtual conductor. This virtual conductor is considered a base for power routing in dc networks; as it can transfer the electric power between nodes at different voltage levels. Furthermore, it allows an easy plug-and-play feature. The proposed bidirectional DC-DC system configuration is investigated analytically, using PSIM simulator, and experimentally.

**Keywords:** bidirectional DC-DC converters, virtual conductor, dc power routing, converter modeling and control.

## I. INTRODUCTION

Nowadays, bidirectional DC-DC converters gain a great attention due to the increasing need to systems with the capability of bidirectional energy transfer between two dc buses. BDCs have various applications that include energy storage in renewable-energy systems, fuel cell systems, hybrid-electric vehicles (HEVs) and uninterruptible power supplies (UPSs) [1-8].

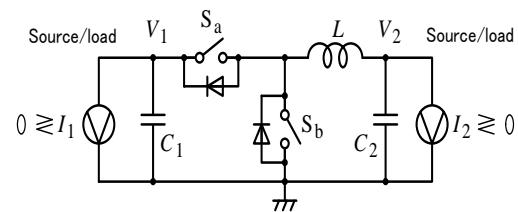
The fluctuation nature of most renewable-energy sources, like wind and solar, makes them unsuitable for standalone operation. A common solution to overcome this problem is to use an energy storage device besides the renewable-energy resource to compensate these fluctuations and maintain a smooth and continuous power flow.

As the most common and economical energy storage devices in a medium-power range are batteries and super-capacitors, a DC-DC converter is usually required to allow energy exchange between storage device and the rest of the system. Such converters must have bidirectional power flow capability with flexible control in all operating modes.

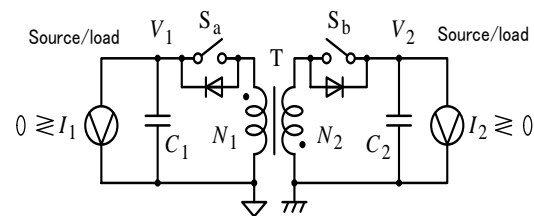
Moreover, when integrating various renewable-energy sources with numerous voltage levels into a dc grid, the main challenge is to have an easy plug and play system with a flexible dc power routing. This system should be capable of integrating such sources at different voltage levels. To face this challenge, a proposed strategy based on a bidirectional DC-DC converter is introduced in this paper.

In this paper, a bidirectional DC-DC converter is investigated and controlled. It is considered that both input and output are independent current sources.

The current source may represent a load, electric double layer capacitors (EDLCs), a battery, or even another bidirectional converter. Therefore, for such converter, it is required to control both  $V_1$  and  $V_2$  to keep the voltage



(a) Non-isolated.



(b) Isolated.

Fig. 1. Circuit examples of a bi-directional DC-DC converter.

difference between them at a certain value regardless of any variation that may be occurred to the currents  $I_1$  and  $I_2$ .

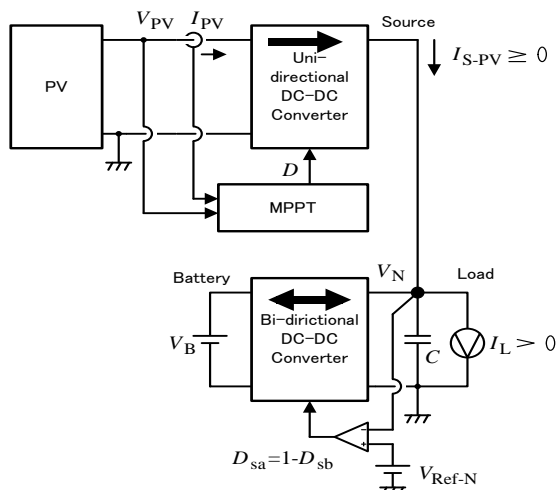


Fig. 2. Using a bi-directional DC-DC converter for charging and discharging of a battery.

## II. BIDIRECTIONAL DC-DC CONVERTER

### A. Circuit examples of a bi-directional DC-DC converter

Basic DC-DC converters such as buck and boost converters (and their derivatives) do not have the bidirectional power flow capability. This limitation is

due to the presence of diodes in their structure, which prevents reverse current flow. In general, a unidirectional DC-DC converter can be turned into a bidirectional converter by replacing the diodes with a controllable switch in its structure [9]. Figure 1 (a) shows an example for a non-isolated bidirectional DC-DC converter, and Fig. 1 (b) shows an example for an isolated bidirectional DC-DC converter.

### B. Using a bi-directional DC-DC converter for charging and discharging of a battery

Figure 2 illustrates an example of a smart house integrates a renewable-energy source (PV) and a storage battery. The PV is connected to the load via a maximum point power tracker (MPPT) and a unidirectional DC-DC converter. While, the battery is connected to the load via bidirectional DC-DC converter; since the power flow between the battery and the load is required to be bidirectional (charge/discharge). The coupling point Voltage,  $V_N$ , is controlled based on  $V_{Ref-N}$ .

## III. DC POWER SYSTEM USING THE PROPOSED BI-DIRECTIONAL DC-DC CONVERTER (THE VIRTUAL CONDUCTOR)

Regarding the aforementioned example in sec. B -Fig. 2- for the sake of having a flexible dc power system; it should be easy to integrate different multi-level voltage sources and loads together. In other words, the coupling point is required to be a multi-level voltages point. The

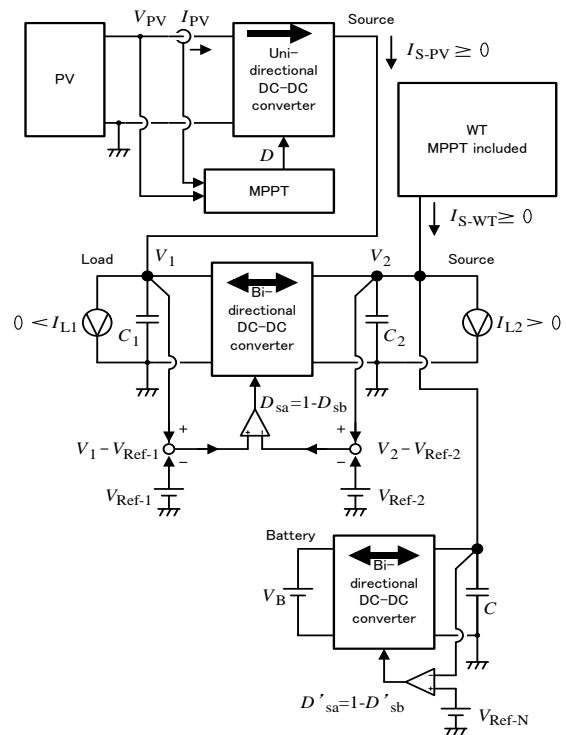


Fig. 3. The proposed bidirectional DC-DC converter as a multi-level voltage coupling point.

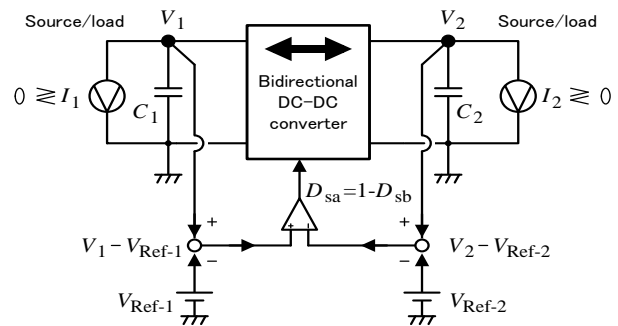


Fig. 4. Implementation of multi-level virtual conductor using a bi-directional DC-DC converter.

bidirectional DC-DC converter, with the proposed control strategy, can play the role of a multi-level voltage coupling point as shown in Fig.3. In this case, the bidirectional DC-DC converter is called a multi-level virtual conductor.

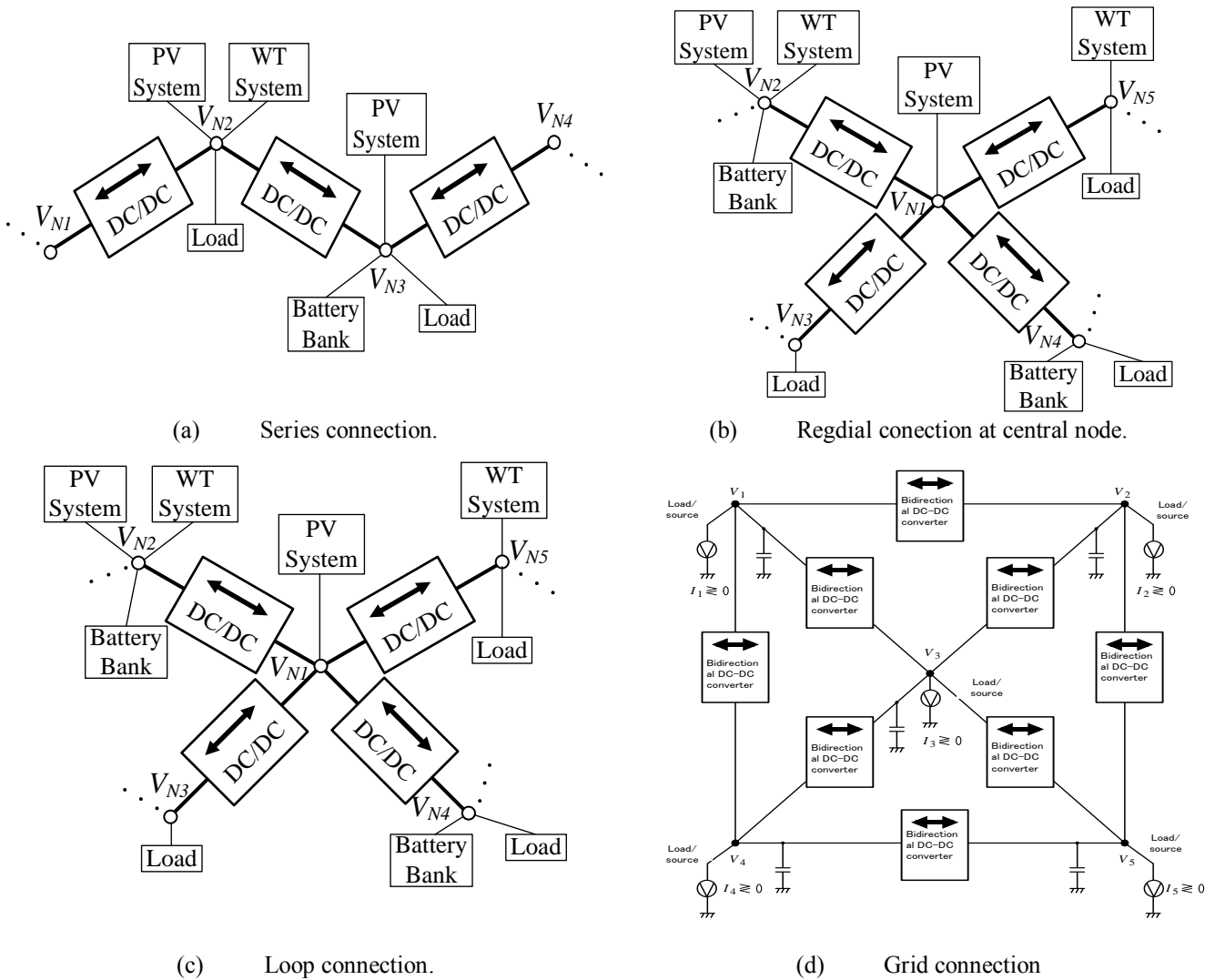


Fig. 5. The configuration examples of the multi-level virtual conductor in dc power system.

A. Implementation of the virtual conductor using a bi-directional DC-DC converter

The proposed control strategy for a bidirectional DC-DC is shown in Fig.4. The main target of this control strategy is to keep the voltage difference between the converter terminals constant at a certain value.  $V_1$  and  $V_2$  are adjusted according to  $V_{Ref-1}$  and  $V_{Ref-2}$  respectively. Therefore, the duty ratios  $D_{Sa}$  and  $D_{Sb}$  of the converter are adjusted to the desired value when  $(V_1 - V_2) = (V_{Ref-1} - V_{Ref-2})$ . Since  $V_{Ref-1}$  and  $V_{Ref-2}$  are constant values; then the difference between  $V_1$  and  $V_2$  is kept constant at the steady state. For the former example of Fig.2 there was only one coupling point ( $V_N$ ), but with this proposed strategy; there are two coupling points  $V_1$  and  $V_2$ .

B. Configuration examples and features of the virtual conductor in dc power system

The virtual conductor allows a flexible power transfer through an energy system having multiple energy sources

with different voltage levels, energy storage equipment, and loads. Factually, it is impossible to use a conductor to connect such an energy system; however, a virtual conductor, having the voltage conversion function of a bidirectional DC-DC converter, can be used.

The configuration examples of the virtual conductor in dc power system are shown in Fig. 5. The series connection is presented in Fig. 5 (a), while the branch connection at a central node is revealed in Fig. 5 (b), and Fig. 5 (c) shows a loop connection. A further complex connection, grid connection, is shown in Fig 5 (d). One practical application of these aforementioned connections can be used in a smart house that integrates different loads and voltages sources together; as shown in Fig. 6. Another practical application can be used in an electrical vehicles (EV) charger substation; as shown in Fig. 7. The features of a dc power system using virtual conductors can be summarized as following:

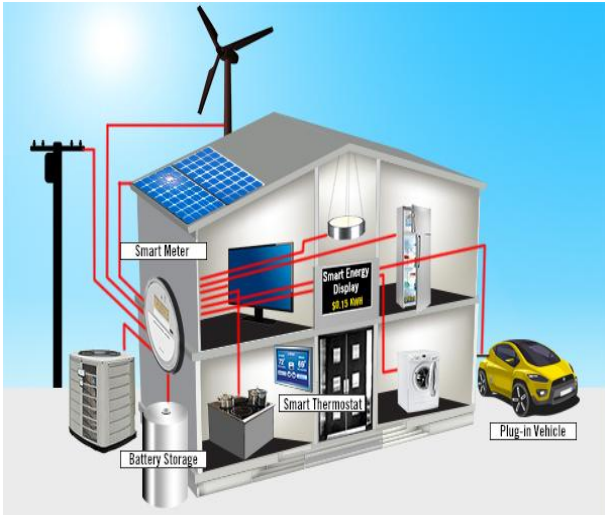


Fig. 6. Smart house integrates different voltage sources and loads



Fig. 7. EV charger substation

1- It is possible to have different voltage levels ( $V_{N1}, V_{N2} \dots$  etc. in Fig. 5).

2- By using the isolated bidirectional DC-DC converter topologies; a galvanic isolation among nodes can be achieved.

3- The virtual conductor allows an easy plug and play of the equipment that is connected to the dc power system; hence the dc power system becomes flexible and reconfigurable.

4- If there is a fault or an accident occurs in one branch or at any node, it is easy to clear this fault by stopping the operation of the related bidirectional DC-DC converter.

5- Regarding Fig. 5 (c), even if there is a fault in one branch, the power will be transferred via the other branch, and this increases the reliability of the dc power system.

#### IV. THE PROPOSED BI-DIRECTIONAL DC-DC CIRCUIT CONFIGURATION

The proposed bi-directional DC-DC circuit configuration is shown in Fig. 8. It employs a DC-DC converter to connect two different Load/supply units. The voltage difference between the converter sides is controlled by the duty ratio of the main switch ( $S_m$ ) and of the synchronously switch ( $S_s$ ). The two bidirectional dc current sources,  $I_1$  and  $I_2$ , have internal resistances,  $r_i$  and  $r_o$ , consequently. There are three storage components:  $C_1$ ,  $C_2$  and  $L$ . Inductor parasitic resistance  $r_l$  and MOSFET turn-on resistance  $r_s$  are included in the model. The transfer function for this converter has been driven based on the state space averaging method [10-15]. Considering the state space vector  $(t) = [v_{c1}(t) \ v_{c2}(t) \ i_L(t)]$ , and the input vector  $u = [I_1 \ I_2]$ ; the state space averaged dc model is shown in (1):

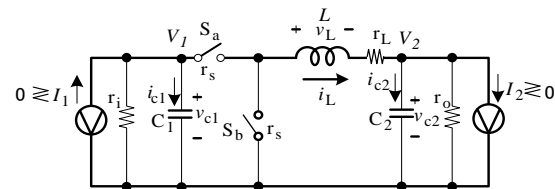


Fig. 8. Circuit configuration of the proposed bi-directional DC-DC converter.

$$0 = A \begin{bmatrix} I_L \\ V_1 \\ V_2 \end{bmatrix} + B \begin{bmatrix} I_1 \\ I_2 \end{bmatrix} \quad (1)$$

where;

$$A = \begin{bmatrix} -\frac{r_s+r_l}{L} & \frac{D}{L} & -\frac{1}{L} \\ -\frac{D}{C_1} & -\frac{1}{r_i C_1} & 0 \\ \frac{1}{C_2} & 0 & -\frac{1}{r_o C_2} \end{bmatrix}, B = \begin{bmatrix} 0 & 0 \\ \frac{1}{C_1} & 0 \\ 0 & -\frac{1}{C_2} \end{bmatrix}$$

By solving (1), the following expressions are resulted:

$$I_L = \frac{r_i D I_1 + r_o I_2}{r_i D^2 + r_o + r_l + r_s} \quad (2)$$

$$V_1 = \frac{r_i I_1 (r_o + r_l + r_s) - D r_o r_i I_2}{r_i D^2 + r_o + r_l + r_s} \quad (3)$$

$$V_2 = \frac{D r_o r_i (I_1 - D I_2) - r_o (r_l + r_s) I_2}{r_i D^2 + r_o + r_l + r_s} \quad (4)$$

The state-space averaged ac model is shown in (5).

$$\frac{d}{dt} \begin{bmatrix} \hat{i}_L \\ \hat{v}_1 \\ \hat{v}_2 \end{bmatrix} = A \cdot \begin{bmatrix} \hat{i}_L \\ \hat{v}_1 \\ \hat{v}_2 \end{bmatrix} + C \cdot \begin{bmatrix} I_L \\ V_1 \\ V_2 \end{bmatrix} \cdot \hat{d} \quad (5)$$

where,

$$A = \begin{bmatrix} -\frac{r_s+r_l}{L} & \frac{D}{L} & -\frac{1}{L} \\ -\frac{D}{C_1} & -\frac{1}{r_i C_1} & 0 \\ \frac{1}{C_2} & 0 & -\frac{1}{r_o C_2} \end{bmatrix}, C = \begin{bmatrix} 0 & \frac{1}{L} & 0 \\ -\frac{1}{C_1} & 0 & 0 \\ 0 & 0 & 0 \end{bmatrix}$$

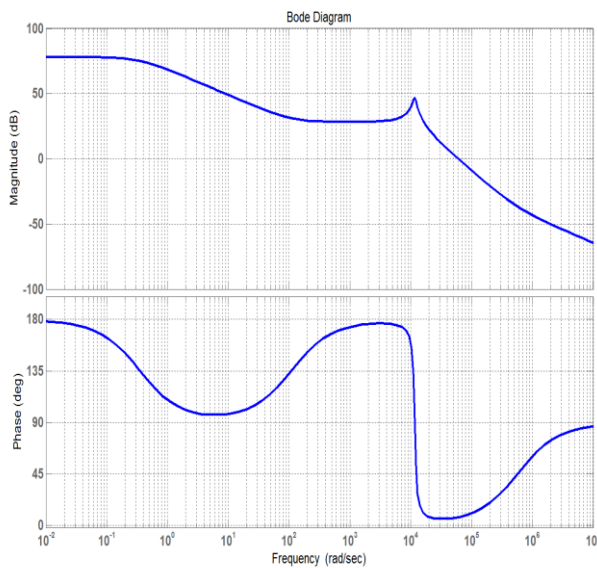


Fig. 9. The frequency characteristics for the control-to-voltage difference transfer function  $G_{ddv}(s)$

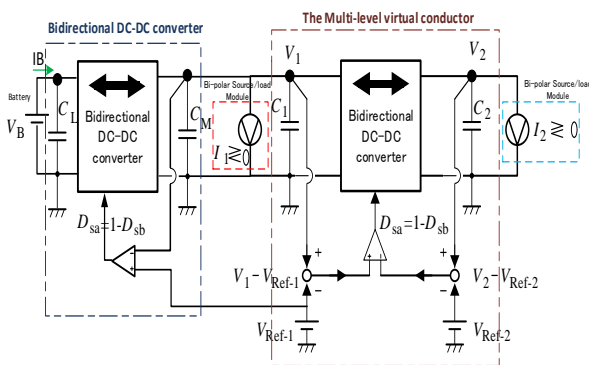


Fig. 10. A prototype dc power system using the virtual conductor

By solving (5), the following equations (6)-(8) are obtained:

$$\hat{v}_1 = \frac{\frac{D}{C_1} \frac{i_L}{s} - \frac{1}{C_1} I_L}{s + \frac{1}{C_1 r_i}} \quad (6)$$

$$\hat{v}_2 = \frac{\frac{1}{C_2}}{s + \frac{1}{C_2 r_o}} \cdot \frac{i_L}{s} \quad (7)$$

$$\frac{i_L}{s} = \frac{\left(s + \frac{1}{C_1 r_i}\right) \cdot \left(s + \frac{1}{C_2 r_o}\right) \frac{V_1}{L} - \frac{D I_L}{C_1 L} \cdot \left(s + \frac{1}{C_2 r_o}\right)}{\left(s + \frac{r_l + r_s}{L}\right) \cdot \left(s + \frac{1}{C_1 r_i}\right) \cdot \left(s + \frac{1}{C_2 r_o}\right) + \frac{D^2 \left(s + \frac{1}{C_2 r_o}\right) + \left(s + \frac{1}{C_1 r_i}\right)}{L C_1}} \quad (8)$$

Using (6)-(8), the control-to-voltage difference transfer function  $G_{ddv}(s)$  can be obtained as in (9), where  $\partial \hat{v} = \hat{v}_1 - \hat{v}_2$ .

$$G_{ddv}(s) = \frac{\hat{v}_1 - \hat{v}_2}{\frac{i_L}{s}} = \left[ \frac{-\frac{D}{C_1}}{\left(s + \frac{1}{C_1 r_i}\right)} - \frac{\frac{1}{C_2}}{\left(s + \frac{1}{C_2 r_o}\right)} \right] \cdot \frac{i_L}{s} - \frac{\frac{I_L}{C_1}}{\left(s + \frac{1}{C_1 r_i}\right)} \quad (9)$$

Figure 9 shows the frequency characteristics for the control-to-voltage difference transfer function  $G_{ddv}(s)$ . To obtain the frequency characteristics for  $G_{ddv}(s)$ , the following parameters are considered:  
 $r_i = r_o = 10 \text{ k}\Omega$ ,  $r_l = 71 \text{ m}\Omega$ ,  $r_s = 150 \text{ m}\Omega$ ,  $L = 80 \text{ mH}$ ,  $C_1 = 330 \mu\text{F}$ ,  $C_2 = 100 \mu\text{F}$ .

## V. TRANSIENT RESPONSE

To investigate the transient characteristics response of the virtual conductor; two 100 watt converters are designed. A prototype dc power system using the virtual conductor is shown in Fig. 10. The virtual conductor is connected at its one end to a bi-polar current source (load/ source), and at the other end to another bi-polar current source and a battery via bidirectional converter. A photo for the experimental setup is shown in Fig.

11. The circuit parameters are shown in Table I. These parameters have been used for both simulation and experimental results. Current waveforms of the bipolar current sources ( $I_1$ ,  $I_2$ ) are intentionally designated to have a stiff change from positive ( $I_1$ ,  $I_2$ ) into negative ( $I_1$ ,  $I_2$ ) to investigate the bidirectional power flow through the virtual conductor. Accordingly, voltages at the bipolar current sources sides ( $V_1$ ,  $V_2$ ) are measured.

The simulation results are shown in Fig. 12, and the experimental results are shown in Fig. 13. From these results, it is obvious that the voltage difference between  $V_1$  and  $V_2$  is kept constant (12 V) regardless of the change in polarities of currents and powers. In other words the virtual conductor has successfully allowed the power to be transferred in both directions between two nodes with a voltage difference in between them.

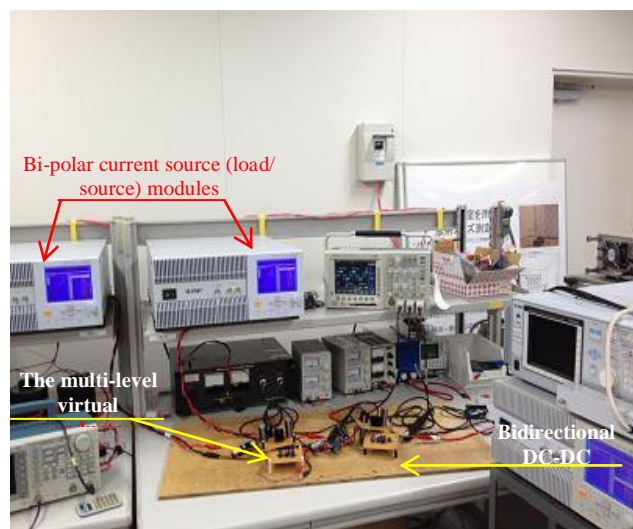


Fig. 11. The experimental test setup



ABLE 1  
 THE CIRCUIT PARAMETERS

Symbol	Description	Value
$V_B$	Battery voltage	48 V
$V_1$	Voltage at node 1	24 V
$V_2$	Voltage at node 2	12 V
$L_1$	Inductance of the first converter	120 $\mu$ H
$L_2$	Inductance of the virtual conductor	80 $\mu$ H
$C_L$	Capacitance at the input of the bidirectional DC-DC converter	100 $\mu$ F
$C_M$	Capacitance at the output of the bidirectional DC-DC converter	200 $\mu$ F
$C_1$	Capacitance at the input of the multi-level virtual conductor	330 $\mu$ F
$C_2$	Capacitance at the output of the multi-level virtual conductor	100 $\mu$ F
$F$	Switching frequency	100 kHz

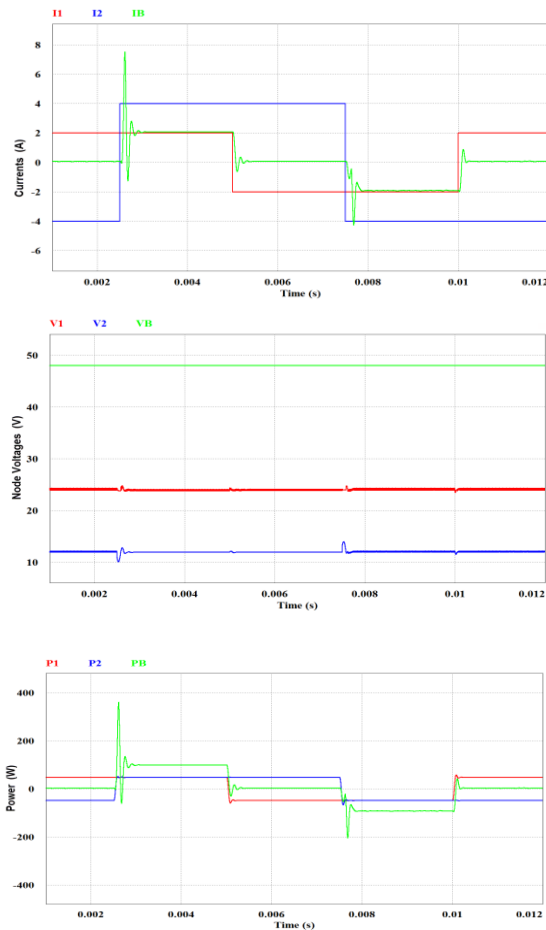


Fig. 12. Simulation result.

## VI. CONCLUSION

This paper proposes a new bidirectional control strategy lead to a performance of a virtual conductor. This virtual conductor is considered a base to power routing in dc networks. It allows an easy plug-and-play feature. This means that any terminal unit (load/source) can be safely and effectively connected / disconnected at its suitable voltage level. The basic idea is presented, an average model

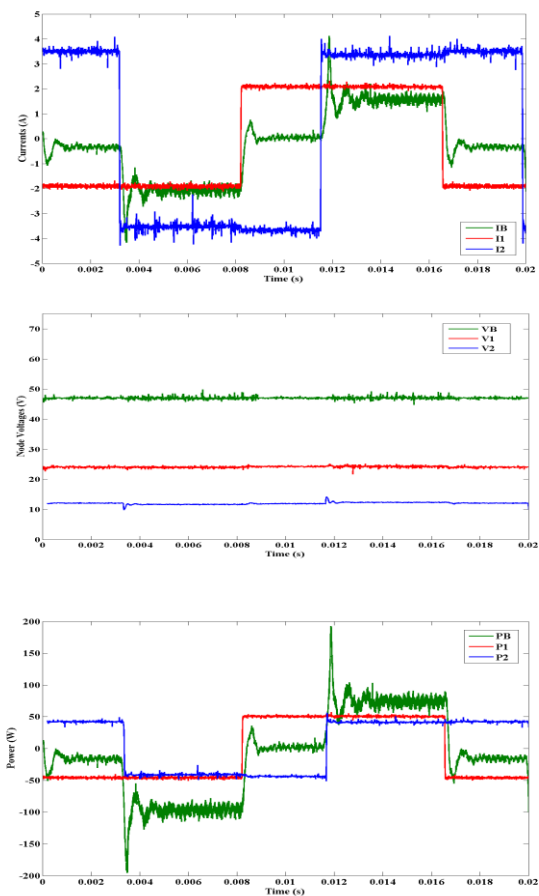


Fig. 13. Experimental results.

contains the bidirectional current sources in both sides is developed, and a representative case study is addressed by simulation and experiment, as well. Both of simulated and experimental results support the basic idea and prove its superiority.

## REFERENCES

- [1] J. Moreno, M.E. Ortuzar, J.W. Dixon, "Energy management system for a hybrid electric vehicle, using ultracapacitors and neural networks," IEEE Trans. on IES, vol. 52, April 2006, pp. 614 – 623.
- [2] M.E. Ortuzar, J. Moreno, J.W. Dixon, "Ultracapacitor-based auxiliary energy system for an electric vehicle: implementation and devaluation," IEEE Trans. on IES, vol. 52, Aug. 2007, pp. 2147 – 2156.
- [3] D.M. Sable, F.C. Lee, B.H. Cho, "A Zero-Voltage-Switching bidirectional battery charger/discharger for the NASA EOS satellite," in Proc. Of APEC, 1992, pp.614-621.
- [4] K. Asano, Y. Inaguma, H. Ohtani, E. Sato, M. Okamura, S. Sasaki, "High performance motor drive technologies for hybrid vehicles," in Proc. of PCC, Nogyo, Japan, April 2007, pp. 1606-1611.
- [5] S. Aso, M. Kizaki, and Y. Nonobe, "Development of fuel cell hybrid vehicles in Toyota," in Proc. of PCC, Nogyo, Japan, April 2007, pp. 1606-1611.
- [6] J. S. Lai, and D.J. Nelson, "Energy Management power converters in hybrid electric and fuel cell vehicles", in Proc. of the IEEE, Vol. 95, No. 4, April 2007, pp. 766 – 777.
- [7] D. P. Urciuoli and C. W. Tipton, "Development of a 90 kW bi-directional DC-DC converter for power dense Applications," in Proc. of IEEE APEC, Dallas, TX., Mar. 2006, pp. 1375–1378.
- [8] P. Jose, N. Mohan, "A Novel Bidirectional DC-DC Converter with ZVS and interleaving for Dual Voltage Systems in Automobiles," in Conf. Rec. of IEEE IAS Annual Meeting, Oct. 2002, pp. 1311–1314.



- [9] D. Dutta, S. Ganguli, "Design of A Bidirectional Dc-Dc Converter for Hybrid Electric Vehicles (Hev) Using Matlab," IJAREEIE, Vol. 2, Issue 7, July 2013, pp. 2994-3002.
- [10] S. Cuk, "Modeling, Analysis, and Design of Switching Converter," Ph.D. thesis, California Institute of Technology, November 1967.
- [11] S. Yang, K. Goto, Y. Imamura, and M. Shoyama " Dynamic Characteristics Model State–space Averaging Method, " in Proc. of INTELEC, 2012, 19.2, pp.1-5, Oct. 2012.
- [12] R. D. Middlebrook and Slobodan Cuk, "A General Unified Approach to Modelling Switching-Converter Power Stages," International Journal of Electronics, Vol. 42, No. 6, pp. 521-550, June 1977.
- [13] Y. Imamura, H. A. Ramadan, Y. Sihun, G.M. Dousoky, M. Shoyama, "Seamless dynamic model for DC-DC converters applicable to bi-directional power transfer," Power Electronics and Applications (EPE), 2013 15th European Conference on , vol., no., pp.1,10, 2-6 Sept. 2013.
- [14] Y. Imamura, H. A. Ramadan, Y. Sihun, G.M. Dousoky, M. Shoyama, "Seamless dynamic model for bi-directional DC-DC converter," IEEE 10th International Conference on Power Electronics and Drive Systems (PEDS), 2013 , pp.1109,1113, 22-25 April 2013.
- [15] H. A. Ramadan, Y. Imamura, Y. Sihun, M. Shoyama, "A New Stability Assessment Criterion For Dc Power Systems Using Multi-Level Virtual Conductors," Fifteenth IEEE Workshop on Control and Modelling for Power Electronics, June 2014.